

## THE ROAD TO DARK ENERGY

DRAGAN HUTERER

*Department of Physics, University of Michigan  
450 Church St., Ann Arbor, MI 48109, USA  
huterer@umich.edu*

I describe and critically evaluate a variety of methods, from simple parametrizations to non-parametric methods, to model the background expansion history in the presence of dark energy. Motivated by these approaches, I review the prospects of determining the properties of dark energy with future experiments, in particular the Dark Energy Survey (DES) and SuperNova/Acceleration Probe (SNAP). Finally, I outline the importance of being able to constrain whole classes of dark energy models, and present recent work that comprehensively studied the observational signature of general scalar field models.

*Keywords:* Cosmology; dark energy; supernovae.

### 1. Introduction

It has now been nearly 10 years since the first solid evidence for dark energy and the accelerating universe. In the intervening years, evidence for the existence of dark energy has strengthened, and there are now multiple lines for evidence for a smooth component that has energy density relative to critical of  $\Omega_{\text{DE}} \approx 0.7$  and the equation of state  $w \approx -1.0$ .

In this talk I review phenomenological methods and strategies that can get us closer to understanding the origin and nature of dark energy.

### 2. Measuring the Expansion History

The primary goal of dark-energy motivated cosmological measurements is to map out the expansion history of the universe. [It is also important to constrain any clustering of dark energy, but such a signal will be extremely difficult to detect even with future experiments, so we do not comment on it any more.]

The “holy grail” of expansion history measurements would be tight constraints on either the dark energy density  $\rho_{\text{DE}}(z)$  or the equation of state  $w(z)$  (complemented with a constraint on  $\Omega_{\text{DE}}$  today) – either function completely specifies the expansion history of the universe and, short of observing clustering of dark energy or its interactions with matter, is the most we can ever do. However, there is a difficulty: typically the observable depends on the wanted quantity  $w(z)$  via a

double-integral relation

$$d_L(z) = (1+z) \int_0^z \frac{dz'}{H(z')}, \tag{1}$$

$$H^2(z) = H_0^2 \left[ \Omega_M(1+z)^3 + (1-\Omega_M) \exp \left( 3 \int_0^z (1+w(z')) d \ln(1+z') \right) \right], \tag{2}$$

where  $d_L(z)$  is the (observable) luminosity distance,  $H(z)$  is the Hubble parameter,  $\Omega_M$  is the matter energy density relative to critical, and we have assumed a flat universe with matter. Therefore, the time-dependent equation of state is a second derivative of the luminosity distance, making it *very* difficult to determine from noisy data.<sup>1</sup> [Note that, while obtaining  $\rho_{DE}(z)$  — essentially the last term in the second equation — only requires the first derivative of distance, understanding of the dynamics of dark energy requires taking a ‘derivative-by-eye’ of the density or, equivalently but better, measuring  $w(z)$ .]

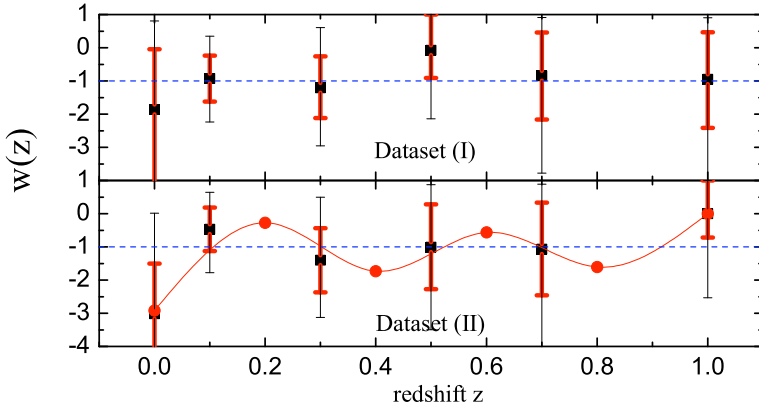


Fig. 1. Constraints on the dark energy equation of state, represented by six values in redshift bins. Adopted from Zhao, Huterer & Zhang (2008).

There are a variety of methods to measure the equation of state of dark energy. Of course one can assume that the equation of state is constant and measure  $\Omega_{DE}$  and  $w = \text{const}$ , but that does not tell us about the dynamics. Most straightforwardly one can generalize this by measuring another parameter that describes the variation of dark energy in redshift, for example  $w(z) = w_0 + w'z^2$  or  $w(z) = w_0 + w_a z / (1+z)$ .<sup>3</sup> More ambitiously, one can attempt to measure the equation of state in several redshift bins and make measurements that are 100% uncorrelated by construction. This method has been pioneered by Ref. 4 (see also Ref. 5); for the most recent results see Fig. 1 which is adopted from Zhao et al.<sup>6</sup>

### 3. Cosmological Probes of Dark Energy

The various cosmological probes of dark energy are displayed in Fig. 2. The solid regions show the (approximate) redshift extent of current surveys, while the hatched regions show future surveys. Type Ia supernovae are the best established probe and still provide the best constraints; weak lensing, baryonic acoustic oscillations and cluster counts are especially promising ones for the near future. As discussed elsewhere at length (e.g. Ref. 7), the cosmic microwave background (CMB) power spectrum mainly serves as a complementary probe, providing measurement of a single quantity (distance to a redshift of  $\sim 1000$  with  $\Omega_M h^2$  essentially fixed).

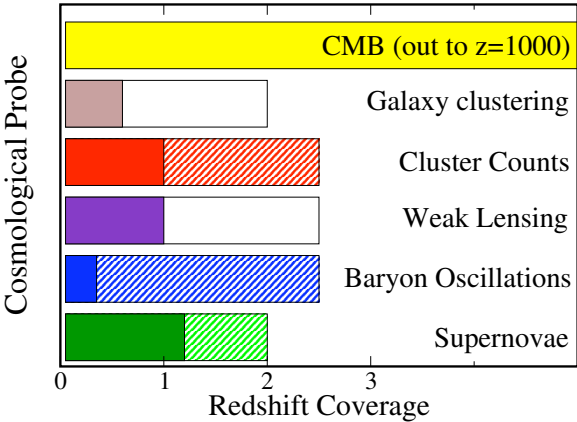


Fig. 2. Principal cosmological probes of dark energy, and their redshift extent for current surveys (solid regions) and future surveys (hatched regions).

### 4. Upcoming Surveys and Experiments

We now briefly review the principal upcoming surveys designed to probe dark energy. The European CMB mission Planck, scheduled for launch in 2008, will provide very important complementary constraints on dark energy mostly due to its better determination of the parameter  $\Omega_M h^2$ . The South Pole Telescope (SPT), a 10-m telescope currently operating on the South Pole, will measure thousands of galaxy clusters via their Sunyaev-Zeldovich signature (scattering of electrons off hot electrons in the cluster) and thus provide constraints on dark energy via the classic number density vs. redshift test. The highly anticipated Large Synoptic Survey Telescope (LSST), an 8m-class telescope expected to be constructed in Chile in the next decade, will primarily provide constraints on dark energy via weak gravitational lensing.

Here we single out and describe in more detail two experiments.

Dark Energy Survey (DES) is a proposal to put a 4-m camera on the Blanco telescope in Chile and perform a survey over 5000 sq. deg. One goal is obtaining

redshifts of clusters identified with the South Pole Telescope. The DES will actually include all of the ‘big four’ probes of dark energy which, in addition to clusters, include observation of type Ia supernovae, weak lensing, and baryon oscillations. DES is planned for construction starting in 2011, and involves an international collaboration of scientists.

SuperNova/Acceleration Probe (SNAP) is perhaps the most ambitious planned experiment to probe dark energy. SNAP is a 2-m space telescope, planned for launch around 2013, and is a candidate for launch as the Joint Dark Energy Mission (joint between the U.S. Department of Energy and NASA). Aided by perfect seeing from space, SNAP will assemble a dataset of type Ia supernovae unprecedented in its control over systematic errors, and over the redshift range  $0.1 < z < 1.7$ . Moreover, SNAP will benefit from the program of weak lensing over an area of 1000 sq. deg which, again because of excellent seeing in space, will have exquisite control of the systematics. Projected constraints from SNAP on the parameters  $\Omega_M$  and  $w = \text{const}$  (left panel) and  $w_0$  and  $w_a$  (right panel) are shown in Fig. 3; in both cases we have assumed a flat universe.

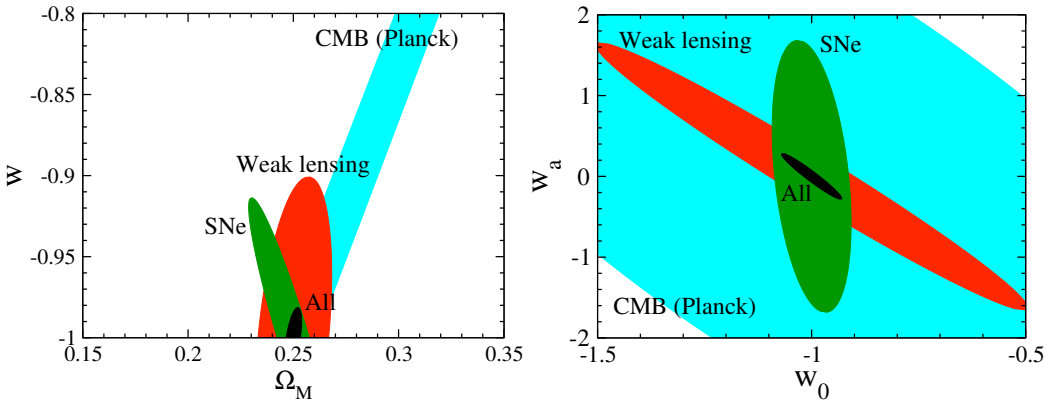


Fig. 3. Projected constraints on  $(\Omega_M, w)$  (left panel) and  $(w_0, w_a)$  (right panel), assuming flat universe, from SNAP.

## 5. Constraints on General Classes of DE Models

### 5.1. Scanning through quintessence models

With the advent of the high quality and quantity of data, it is important to have reliable ways of scanning through whole classes of dark energy models, and determine which ones are ruled out and which are not. More importantly, it is important to be able to establish whether the class of models itself imposes a constraint on the range of dark energy histories. We now describe one such approach, established by Huterer & Peiris<sup>8</sup> (for a related work, see Ref. 9).

We have adapted the flow-roll formalism from inflation (e.g. Ref. 10) to the case of dark energy. Unlike in inflation, there are *no* small parameters with dark

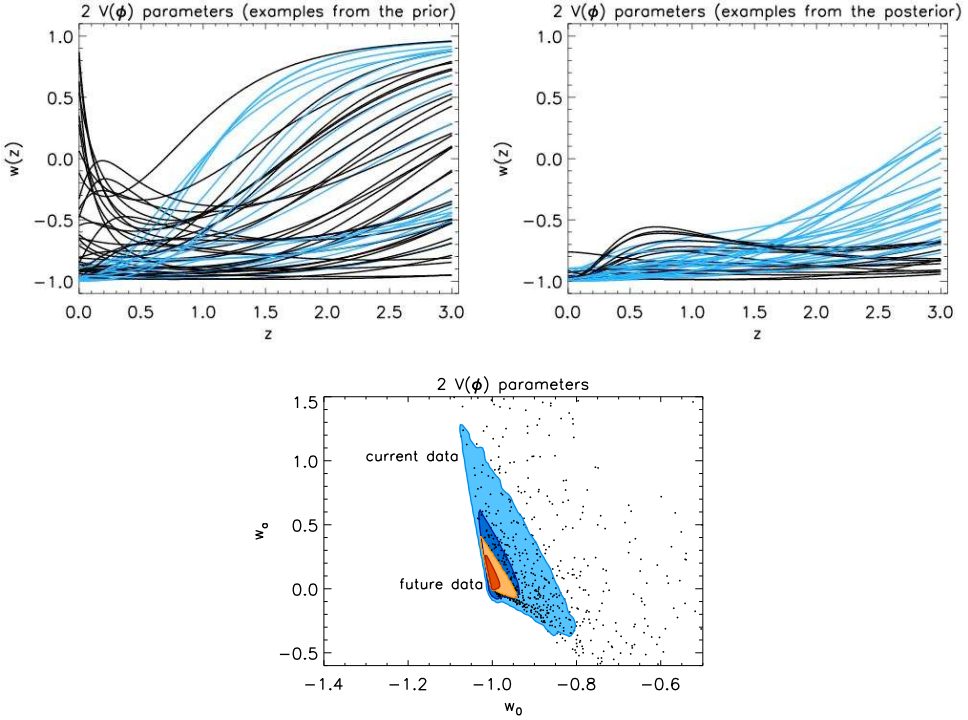


Fig. 4. Top left panel: representative histories  $w(z)$  for a number of randomly chosen sets of initial conditions, shown for illustration without applying cosmological data constraints. Models which are freezing are color-coded in blue, while the models color-coded in black are neither thawing nor freezing. We find that thawing models are very rare. Top right panel: evolution histories of a number of models which were accepted steps in the MCMC. Therefore, whereas the left panel shows examples of models generated by the *prior*, the right panel shows examples of models in the *posterior*. Bottom panel: 68% and 95% CL constraints on  $w_0$  and  $w_a$  from current data and future data; points represent a small subsample of representative scalar field models considered. Adopted from Huterer & Peiris (2007).

energy, and thus the approach is necessarily less general – we have to specialize in a specific class of quintessence potentials, for example, second or third order polynomials  $V(\phi)$ . With that class of models chosen, we run through all models in the class – in practice, this means choosing the initial conditions for all parameters millions of times, computing the dark energy history for each model, and confronting it with the data.

Figure 4 (top row) shows expansion histories (or,  $w(z)$ ) for a (small) subsample of second order polynomial models. The top left panel shows the histories in the prior – before comparison with the data – while the top right panel shows the same models in the posterior, so those that have survived the data cut. Note that models in the prior cover a very wide range of dark energy histories, even those that are obviously ruled out. Here we have used the current data from type Ia supernova, baryon acoustic oscillation, and CMB anisotropies.

The bottom panel of Fig. 4 shows constraints on the  $w_0$ - $w_a$  plane for models in our posterior. [Defining and computing the parameters  $w_0$  and  $w_a$  from our models'  $w(z)$  is described in Ref. 8.] Note several features. First, the constraints have a characteristic triangular shape. The lower two edges of the ‘wedge’ are due to the fact that scalar field models have  $w(z) \geq -1$ . The third, top edge is one that improves as data improve, and models lying outside of the constraints are apparent. What is also clear is that some of our scalar field models approach the cosmological constant case ( $w_0 = -1$ ,  $w_a = 0$ ) arbitrarily close. Finally, note that future constraints will have an area in the  $w_0$ - $w_a$  plane about 10 times better than current constraints — in other words, their Figure of Merit (introduced in Refs. 11, 12) will be that much better.

## 5.2. Thaw or freeze?

Caldwell and Linder<sup>13</sup> have pointed out that scalar field models naturally fall in classes of “thawing” or “freezing” depending on whether they are asymptotically receding from or approaching the state of zero kinetic energy where the equation of state is  $-1$ .

With the benefit of our framework we can quantitatively answer questions about the division of models. Our parametrization is more general than that in most previous studies as we consider all quadratic/cubic polynomials for  $V(\phi)$  with maximally uninformative priors for the initial speed and energy density of the field. For each models from our Markov Chains, we determine whether it is thawing (so that  $w$  increases in time), or freezing ( $w$  decreases in time), or neither.

Figure 5 shows that our models often do not lie solely in either thawing or freezing region, nor do they necessarily retain their purely thawing or freezing behavior. This remains true even if we only restrict to very late-time evolution ( $z < z_* = 1$ , say). Figure 5 also shows a thick (pink) line, a more general lower bound<sup>14</sup> which is obeyed by all monotonic quintessence potentials. This latter bound, unlike the one from Ref. 13, is obeyed by all our models except for those where the field samples a section of the potential that is not monotonic. As described in Ref. 8 in detail, the disagreement between our models and the phenomenologically expected bounds from Ref. 13 is due to the interplay between the initial conditions of the scalar field, the effects of Hubble friction, and the shape of the effective potential (specifically, non-monotonicity in the second derivative) that our more general class of models possesses.

## 6. Conclusions

We have discussed the present status of the quest for dark energy and future prospects. We already have interesting constraints on the equation of state  $w(z)$  parametrized in several redshift bins; future constraints will be a factor of a few better. We eagerly await a variety of promising experiments, including ground-based

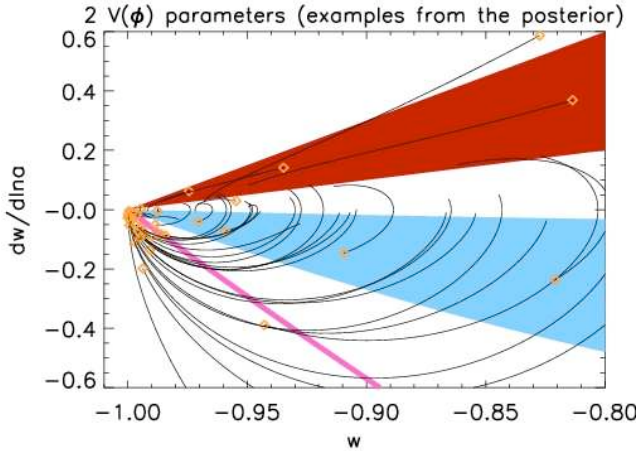


Fig. 5. Trajectories in the  $w - dw/d\ln a$  plane, together with shaded regions that should be occupied by thawing and freezing models according to Caldwell & Linder, the orange diamonds denoting  $z = 0$ . Our models often do not lie solely in either region, nor do they necessarily retain their purely thawing or freezing behavior. Reasons for the disagreement are discussed in the text. The thick (pink) line shows a more general lower bound on monotonic quintessence potentials from Scherrer which is obeyed by all our models satisfying this assumption. Adopted from Huterer & Peiris (2007).

surveys such as DES and LSST, and space-based surveys such as SNAP. We also pointed out the importance of *general* classes of dark energy models, and presented as an example work of Huterer & Peiris.

The future of dark energy measurements is bright and we are very likely to learn a lot about our universe. Whether we will reveal the physical nature of dark energy, however, remains to be seen.

## Acknowledgments

I would like to thank the organizers of the CosPA 2007 meeting for the invitation and for hosting a wonderful and stimulating workshop.

## References

1. D. Huterer and M. S. Turner, *Phys. Rev. D* **60**, 081301 (1999).
2. A. R. Cooray and D. Huterer, *Astrophys. J.* **513**, L95 (1999).
3. E. V. Linder, *Phys. Rev. Lett.*, **90**, 091301 (2003).
4. D. Huterer and A. Cooray, *Phys. Rev. D.*, **71**, 023506 (2005).
5. Y. Wang and M. Tegmark, *Phys. Rev. Lett.*, **92**, 241302 (2004).
6. G. Zhao, D. Huterer, and X. Zhang, *Phys. Rev. D*, submitted, arXiv:0712:2277.
7. J. Frieman, D. Huterer, E. Linder, and M. Turner, *Phys. Rev. D*, **67**, 083505 (2003).
8. D. Huterer and H. V. Peiris, *Phys. Rev. D*, **75**, 083503 (2007).
9. M. Sahlen, A. Liddle, and D. Parkinson, *Phys. Rev. D* **72**, 083511 (2005).
10. M. Hoffman and M. S. Turner, *Phys. Rev. D* **65**, 023506 (2001).

11. D. Huterer and M. S. Turner, *Phys. Rev. D* **64**, 123527 (2001).
12. A. Albrecht *et al.*, arXiv:astro-ph/0609591.
13. R. Caldwell and E. V. Linder, *Phys. Rev. Lett* **95**, 041301 (2005).
14. R. Scherrer, *Phys. Rev. D* **73**, 043502 (2006).